Physics with CDF Small Angle Spectrometer

Ettore Focardi
INFN and Scuola Normale Superiore
Pisa - Italy

1. Introduction

I describe here the small angle spectrometer[1] that CDF intends to use to accomplish the following physics goals:

1) a measurement of the elastic scattering differential cross section $d\sigma/dt$, in the region $0.04 < |t| < 2\ (\mathrm{GeV}/c)^2$;

2) a measurement of the total cross section σ_T and of the machine luminosity;

3) a measurement of the differential cross section $d^2\sigma/dtdM^2$ for proton single diffraction dissociation $\bar{p}p \rightarrow \bar{p}M$ in the region $0.04 < |t| < 0.4\ (\mathrm{GeV}/c)^2$ and $M^2 < 0.1$ s ($M \lesssim 600$ GeV for $\sqrt{s}=2000$ GeV);a similar study for $\bar{p}p \rightarrow pM$ will also be performed;

4) a search for special events associated with high mass diffraction dissociation;

5) a study of the double-pomeron process $\bar{p}p \rightarrow \bar{p}pM$ at small t and $M^2 \lesssim 0.01$ s.

A short description of how each measurement will be performed is given in the following. Measurements 1), 2), 3), except for hight-t elastic scattering, will be performed with the Collider operating at high β ; thus smaller scattering angles and smaller t-values will be reachable. Some aspects of the double Pomeron process can also be measured in the high β operating mode (2). Elastic scattering in the region $0.4 \lesssim |t| \lesssim 2\ (\mathrm{GeV}/c)^2$ and a search for diffractively produced large mass special events will be done at low β to take advantage of the increased machine luminosity and the longer running time.

2. The Detector

The detector is made out of 26 silicon detectors placed in 7 stations, S_1 trough S_7 along the beam line, a sketch is shown fig. 1. The silicon wafers are located inside the beam pipe and can be remotely moved as close as possible to the beam during running time. Three different types of wafers are foreseen for two different types of insertions.

a) In S4, S5 no accurate adjustement of the distance of the crystals from the beams is required; the crystals are simply flipped-in for data taking, fig. 2 shows the mechanical design. Six petals 60° wide in azimuth are included in each insertion (fig.3). Each petal has 32 strips (concentric arcs) around the beam axis, covering the region 1 mrad $< \vartheta <$ 6 mrad or $5.6 < |\eta| < 7.6$. On the back side each petal is divided into 8 φ-pads. In the closed position, when the crystals are perpendicular to the beam, the inner hole which is left open has a radius of 6 mm, corresponding to $\sim$15 times the beam width. In the open position the crystals are parallel to the beam.

b) Four half-moon silicon detectors are inserted, two per station, in S_3, S_6 having 16 ϑ-electrodes and 8 φ-pads (fig.4). They cover the angular range 0.2 mrad $< \vartheta <$ 1 mrad or $7.6 < |\eta| < 9.2$. During the high β runs the half moons are fully closed and have 15 mm left as inner diameter hole. Table I gives the beam size at various locations.

c) The third wafer shape is a rectangle of 36x30 mm^2. There are two such detectors per station in S_1, S_2, S_3, S_6, S_7. They have 64 vertical electrodes and 32 horizontal pads (fig.5).

S_1, S_2 measure the antiproton momentum (S_3 is also involved at large momentum transfers), employing a set of accelerator bending magnets as well as some quadrupoles. S_6, S_7 measure the proton momentum employing only a set of accelerator quadrupoles. In S_1, S_2 the position resolution in the x-direction, which determines the momentum resolution, is 50 μm. Stations S_4, S_5 together with beam-beam scintillation counters C_4, C_5 (see in fig.1) provide a double-arm beam-beam trigger and serve as a luminosity monitor. Table II gives a summary of the shape and number of electrodes of the detectors of the various stations. Four petal prototypes are presently under test in the Tevatron ring. The test assembly is shown in fig.6.

3. Elastic Scattering

The elastic scattering will be measured using the rectangular detectors S_1, S_2, S_3 and S_6, S_7.

The good event will be selected by requiring collinearity between the two arms, and the momentum in each arm to be equal to the beam momentum.

The expected momentum resolution is 0.1% for antiprotons while for protons due to the lack of bending magnet in the p-line it is only 1%.

The t-resolution is determined by the beam divergence. The expected σ_{rms} is[3] 0.003 $(GeV/c)^2$ at $|t| = 0.1\ (GeV/c)^2$ in high β and 0.08 $(GeV/c)^2$ at $|t| = 1\ (GeV/c)^2$ in low β.

At small t-values the differential cross section $d\sigma/dt$ can be written as $\frac{d\sigma}{dt} = (\sigma^2/16\pi)e^{bt}$.

Since $\sigma_T \simeq 65$ mb and $b \simeq 18\ (GeV/c)^{-2}$ at $\sqrt{s} = 2$ TeV, with a luminosity of $10^{28}\ cm^{-2}\ sec^{-1}$ (at high β), about 10^4 events/hour will be collected in average in the 0.01 $(GeV/c)^2$ wide detector bins in the range $0.04 < |t| < 0.1\ (GeV/c)^2$. At $|t| \sim 0.4\ (GeV/c)^2$ the expected rate is 10^2 events/hour. With these rates $(d\sigma/dt)_{t=0}$ can be determined with a statistical precision of

1% in a few hours. At large t and at s=2 TeV, the diffraction minimum is expected to appear at $|t| \sim 0.7$ $(GeV/c)^2$, with a cross section $d\sigma/dt \simeq 10^2$ $mb(GeV/c)^{-2}$; thus with $\mathcal{L} \sim 10^{30}$ cm^{-2} sec^{-1} (low β) about 150 events/hour per 0.01 $(GeV/c)^2$ are expected in S3, S6 in the range $0.5 \lesssim |t| \lesssim 1$ $(GeV/c)^2$. Also the diffraction minimum can thus be studied in a short time. With a total integrated luminosity of 10^{36} cm^{-2} we expect $\sim 2 \cdot 10^3$ events per 0.01 $(GeV/c)^2$ at $|t| = 2$ $(GeV/c)^2$.

4. Single Diffraction

The differential cross section for the process $\bar{p}p \to \bar{p}X$ can be estimated as[4] $d^2\sigma/dt\, dM^2 = (0.68/M^2)12e^{12t}$. The process signature will be a leading antiproton in coincidence with one or more charged particles in the other hemisphere. The events are assumed to originate at the center of the beam-beam average region, and the $\bar{p}$ momentum is measured by stations S_1, S_2. In a number of cases also S_3 may be hit, providing an additional constraint to the event. The acceptance at high β is greater than 50% for $0.04 \lesssim |t| \lesssim 0.4$ $(GeV/c)^2$ and $M^2/s \lesssim 0.1$. At low β the acceptance is large for $|t| \gtrsim 0.4$ $(GeV/c)^2$ which compensates for the smaller cross section. The t-dependence of the cross-section can thus be well studied at all t's. After including a modest extrapolation at t=o the total diffractive cross-section can thus be obtained. The 'missing mass' resolution is $\Delta M/M = \frac{1}{2} \cdot \Delta p/p.s/M^2$, at $M^2/s = 0.05$ we expect $\Delta M/M \sim 1 - 3\%$ corresponding to $\Delta p/p$ $0.1 - 0.3\%$. As mentioned already, on the proton side the momentum is measured by S_6, S_7 with an expected accuracy of $\sim 1\%$. This resolution is poor, but still allows an useful comparison to be made between antiproton and proton diffraction at $|t| > 0.4$ $(GeV/c)^2$.

The charged particles of the dissociating proton may trigger C_5, S_5, S_6. A study of the angular distribution of those events will allow to extimate by extrapolation the loss events at angles larger than the maximum angle or smaller than the minimum angle covered by the detector. In ref.4 an estimate is obtained of .8% end 1.2% for the respective losses. A correction for these losses will be applied when deriving the total cross-section.

At low t, all cross sections are large and the acceptance of S_1,S_2 is also good. Therefore the search for special events in single diffraction will be done as a function of M using S_1, S_2 at low β [5].

5. The Total Cross-Section σ_T Measurement

The total cross section σ_T will be measured in a luminosity indipendent method[6]. This method consists in measuring simultaneously the forward elastic scattering and the total interaction rates

$$\sigma_T = \frac{N_T}{L} = \frac{N_{el} + N_{in}}{L} \qquad \sigma_T = \frac{16\pi}{1+\rho^2} \frac{\left(\frac{dN_{el}}{dt}\right)_{t=0}}{N_{el}+N_{in}}$$

where ρ is the ratio of the real to the imaginary part of the forward nuclear scattering amplitude. For $\sqrt{s}$ = 2 TeV extrapolated values for ρ are in the range $0.094 < \rho < 0.161$, thus the factor $1+\rho^2$ is only a $\sim$ 1% correction. The inelastic and elastic rates will be measured simultaneously at high β. The trigger could be the coincidence

$$(S_1+S_2+S_3+S_4+C_4) \cdot (C_5+S_5+S_6+S_7)$$

The elastic and inelastic events will be sorted out in the off-line analysis. We expect to reach a σ_T accuracy of $\sim$ 2%[3].

6. High Mass Diffraction Studies

Special events in the process $\bar{p}p \rightarrow \bar{p}X$ will be searched for at low β, tagging the diffracted proton mass in the $\bar{p}$ spectrometer. One can predict the mass spectrum accepted by S_1, S_2, as shown in fig. 7[7]. The shape of the spectrum can be understood in terms of the following relations:

$$\frac{d^2\sigma}{dt\,dM^2} \sim \frac{e^{bt}}{M^2} \qquad p = p_0 (1 - M^2/s)$$

where p is the $\bar{p}$ recoil momentum. The first decrease ($M_x < 100$ GeV) is due to the increasing mass; however, with increasing $\bar{p}$ inelasticity lower t-values are bent into S_1, S_2 and cause the acceptance to increase again. In total, the accepted cross-section at $M \geq 300$ GeV can be estimated to be 0.5 mb. This cross section is large to allow a search for new heavy particles (e.g. new flavours) possibly produced in diffraction above some mass threshold[5].

References

1) S.Bertolucci et al., CDF-Note 278 (1985)

2) S.Belforte et al., CDF-Note 262 (1984)

3) F.Bedeschi et al., CDF-Note 215 (1984)

4) S.Belforte et al., CDF-Note 257 (1984)

5) G.Bellettini, Aspen Winter Physics Conpherence series 1985, INFN PI/AE 85-1

6) G.Bellettini et al., CDF-Note 59 (1981)

7) F.Bedeschi, CDF-Note 270 (1985)

Figure captions

1) Plan view of the small angle silicon detector system of CDF

2) Engineering drawing of the vacuum inserts S_4, S_5

3) Polar and azimuthal electrode structure of the silicons at S_4, S_5

4) Half moon detectors for insertions S_3, S_6

5) Electrode structure of the rectangular silicon at $S_{1,2,3,6,7}$

6) Photograph of the prototype telescope of silicon 'petals'

7) Accepted partial cross section of diffractive events

TABLE I

Beam size in mm at various locations

Location	High β ϑ_x	High β θ_y	Low β ϑ_x	Low β θ_y
S4	0.45	0.48	0.36	0.34
S5	0.49	0.45	0.37	0.36
S3	0.50	0.50	1.60	0.52
S6	0.48	0.52	0.57	1.53

TABLE II

Detector Types and Channels

Detector type	Bins per wafer	Wafers per station	Stations	Number of Channels
Petal	$32\theta + 8\varphi$	6	S4 S5	(32 + 8)+6 + 2= 480
Half-moon	$16\theta + 8\varphi$	2	S3 S6	(16 + 8)+2 ± 2= 96
Rectangle	64x + 32y	2	S1 S2 S3 S6 S7	(64 + 32)=2 + 5= 960
			Total number of channels	=1536

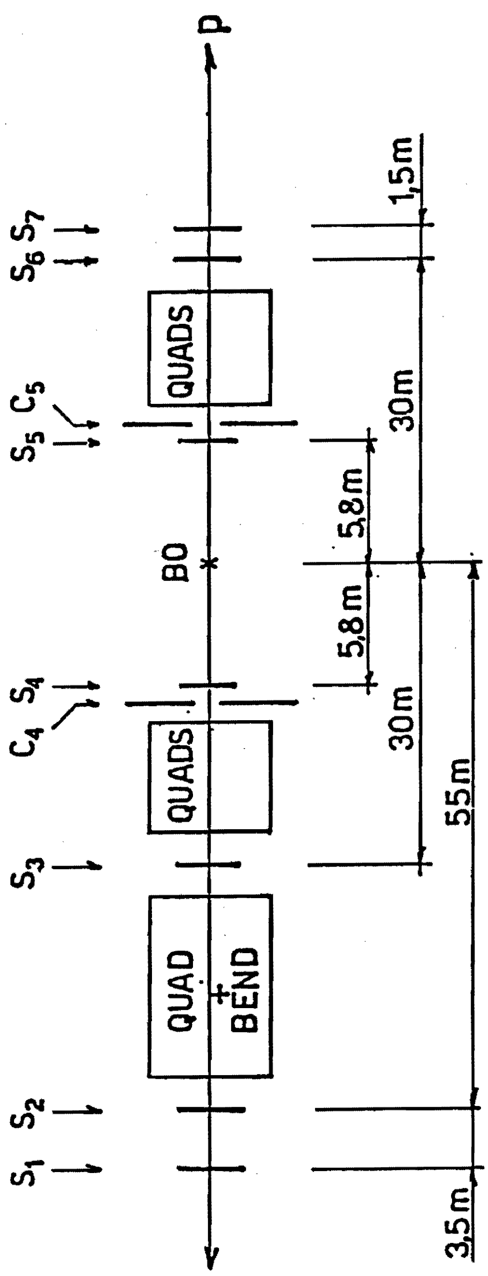
$\bar{p}$
p
S_1
S_2
QUAD
+
BEND
S_3
QUADS
C_4
S_4
BO
S_5
C_5
QUADS
S_6
S_7
3,5m
55m
30m
5,8m
5,8m
30m
1,5m

Fig. 1

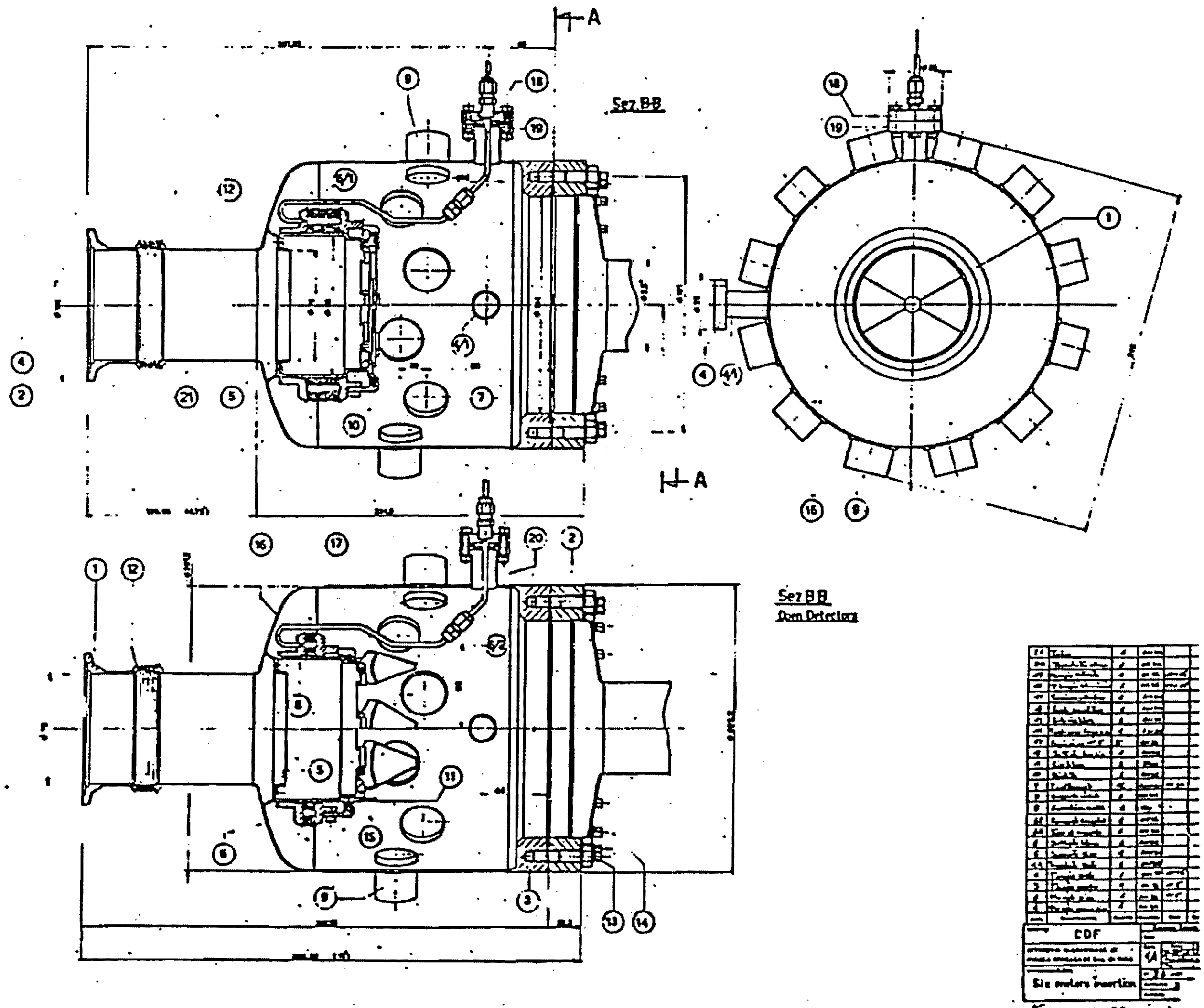

Fig.2

S_4 S_5 "petals"

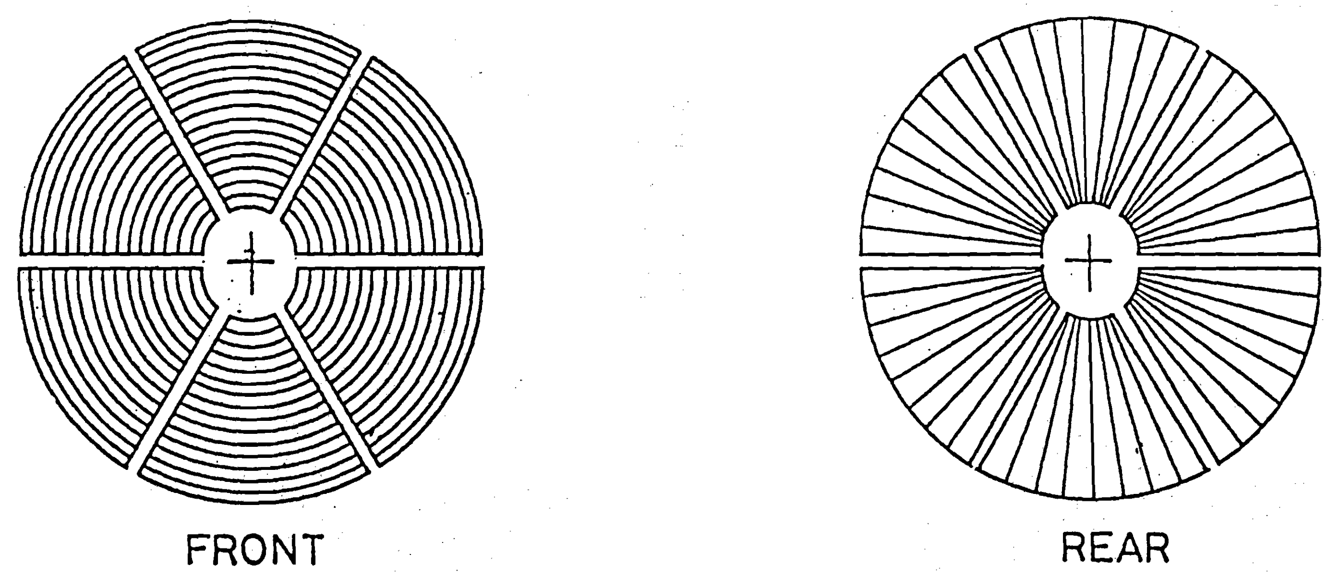

Fig. 3

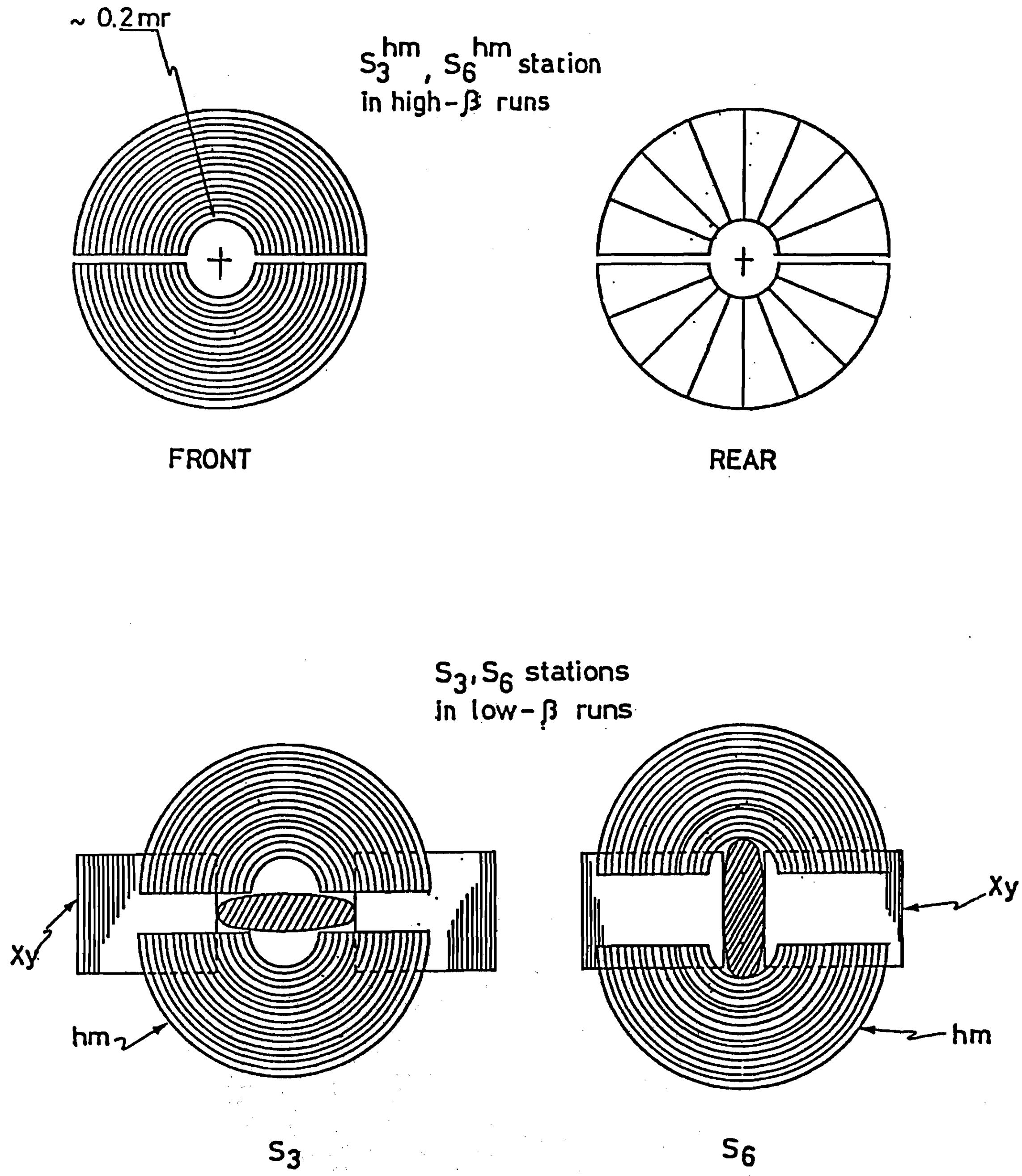
~ 0.2mr
S_3^{hm}, S_6^{hm} station
in high-β runs
FRONT
REAR
S_3, S_6 stations
in low-β runs
Xy
hm
Xy
hm
S_3
S_6

Fig. 4

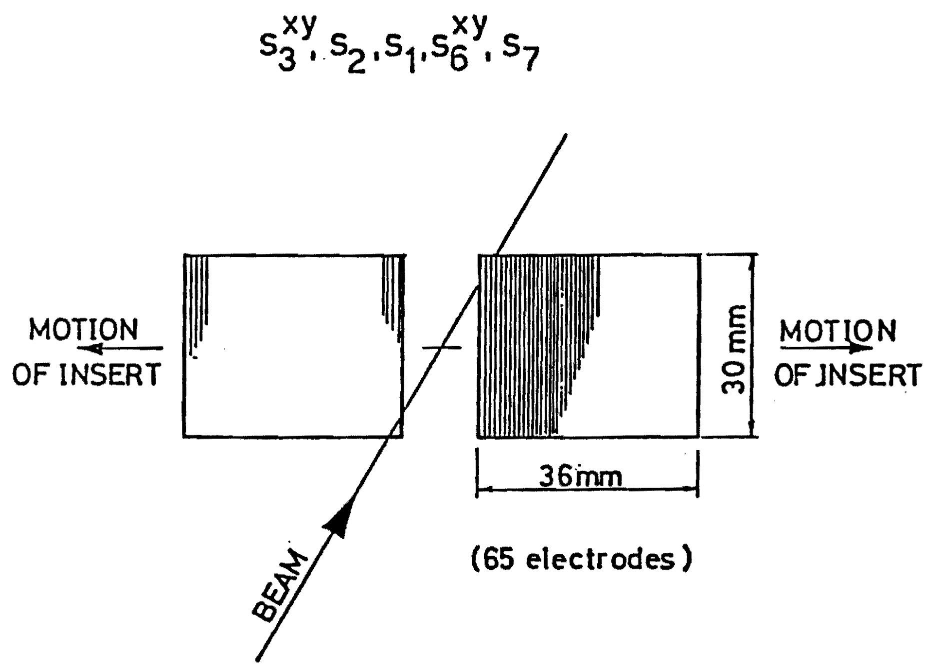
$S_3^{xy}, S_2, S_1, S_6^{xy}, S_7$
MOTION
OF INSERT
MOTION
OF INSERT
30 mm
36mm
(65 electrodes)
BEAM

Fig. 5

Fig. 6

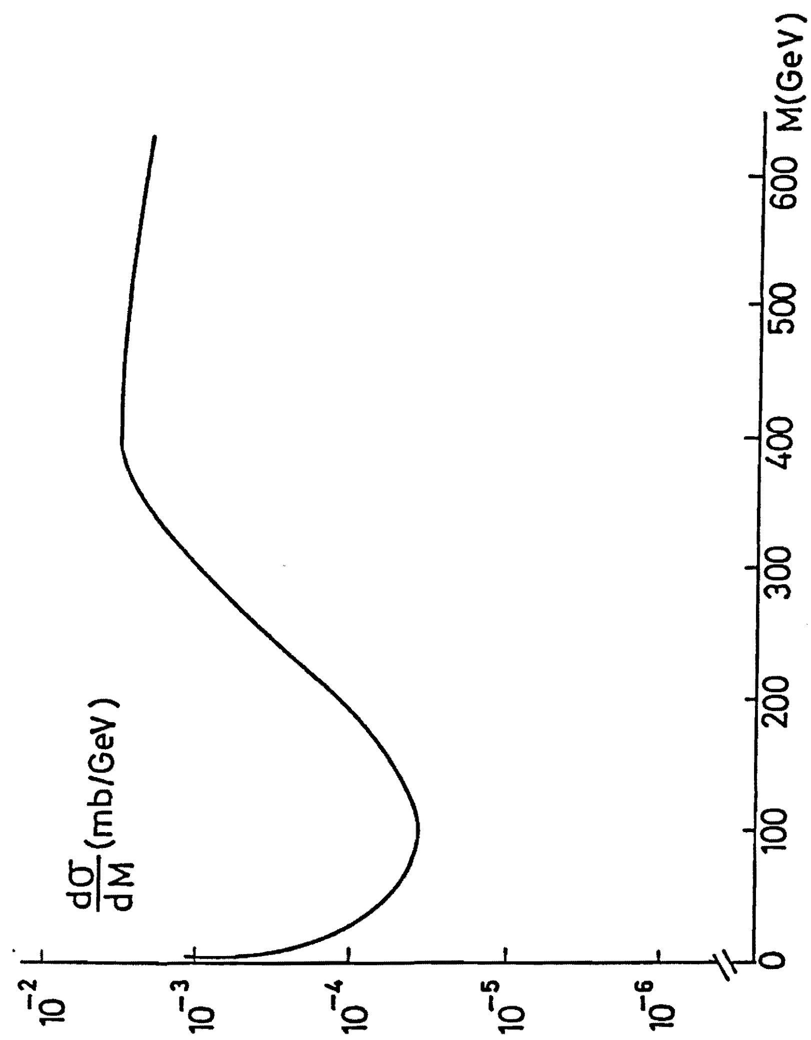

Fig. 7